

Determining the compression behaviour of pharmaceutical powders from the force–distance compression profile

Osmo Antikainen^{a,*}, Jouko Yliruusi^{a,b}

^a *Pharmaceutical Technology Division, Viikinkaari 5 E, University of Helsinki, Helsinki 00014, Finland*

^b *Viikki Drug Discovery Technology Center, University of Helsinki, Helsinki 00014, Finland*

Received 5 August 2002; received in revised form 4 December 2002; accepted 5 December 2002

Abstract

The force–displacement curves obtained from an eccentric tablet machine were examined in a new way. The tendency of the material for plastic deformation, fragmentation and elasticity is expressed as numerical values, which are comparable between different materials. The dependence of these numerical values on the compression pressure was modelled. The accuracy of the displacement measurement was improved by filtering out noise from the measurement data by a novel method. The plastic deformation of the material near the force maximum of the compression cycle could be seen accurately from this precise displacement data. The elastic deformation of the tablet machine was also defined very precisely from the running machine. Tablets were made with an eccentric tablet machine using fixed lower and upper punch adjustments. This ensured that the speed of the upper punch and the theoretical height of the tablets were the same for all compactions. Therefore, only the properties of the materials determined the differences in the shape of the compression curves. The test materials used were α -lactose monohydrate, two grades of microcrystalline cellulose, maize starch and dicalcium phosphate dihydrate. The results showed that the use of accurate displacement measurement is essential in order, to see the small variations in the shape of the force–displacement curve near the force maximum of the compression cycle, and it made it possible to dynamically calibrate the elastic deformation of the eccentric tablet machine during compression. It turned out that the numerical values obtained with the new method described the plastic, brittle and elastic properties of the tested materials satisfactorily in a wide compression pressure range.

© 2002 Elsevier Science B.V. All rights reserved.

Keywords: Plasticity; Fragmentation; Elasticity; Force–displacement profile; Displacement measurement; Eccentric tablet machine

1. Introduction

All materials used in tableting vary in their mechanical behaviour during compression. Materials like magnesium carbonate, calcium carbonate, calcium phosphate, crystalline lactose, sucrose and dibasic calcium phosphate dihydrate are considered to consolidate mainly by fragmentation (Armstrong and

Haines-Nutt, 1970; McKenna and McCafferty, 1982; Roberts and Rowe, 1985). Ductile materials that consolidate by plastic deformation are, e.g. microcrystalline cellulose, stearic acid (David and Augsburger, 1977; Roberts and Rowe, 1986), sodium chloride (Duberg and Nyström, 1982) and starch (Hardman and Lilley, 1970). All materials, however, possess both an elastic and a plastic component. The volume reduction mechanism that dominates for a specific material is also dependent on factors such as temperature, compaction rate and particle size. Lower temperatures and faster loading during compression will

* Corresponding author. Tel.: +358-191-59146;

fax: +358-191-59144.

E-mail address: osmo.antikainen@helsinki.fi (O. Antikainen).

generally facilitate consolidation by fragmentation (Roberts and Rowe, 1985, 1986). Particle size seems to affect mainly the compression properties of brittle materials (Roberts and Rowe, 1987). Pharmaceutical materials normally consolidate by more than one of these mechanisms (Duberg and Nyström, 1986). Therefore, there is a need for a general method which is able to classify reliably the compaction behaviour of different materials. It is particularly important to know the extent of the plastic and brittle behaviour of materials at various compression levels.

The mathematical analysis of compaction profiles was first proposed by Long in 1960 (Watt, 1988), and was essentially derived from powder metallurgy. Numerous new methods have been developed for this purpose since that (Heckel, 1961a,b; Cooper and Eaton, 1962; Kawakita and Tsutsumi, 1966; Dietrich and Mielck, 1983). The Heckel equation is probably the most widely used compaction profile formula in the field of tablet making. It has also been developed for use in powder metallurgy and its suitability for pharmaceutical powders is sometimes questionable (Pedersen and Kristensen, 1994; Sonnergaard, 1999). Considerable care is needed in the interpretation of compaction profiles, and usually their use must be restricted to the machine on which they are generated.

2. Materials and methods

2.1. Test materials

The test materials used were 80-mesh α -lactose monohydrate (EMW, Verghel, the Netherlands), two grades of microcrystalline cellulose (Avicel® PH-101 and PH-200; FMC International, Cork, Ireland), maize starch (National Starch & Chemical GmbH, Neustadt, Germany) and dicalcium phosphate dihydrate (Calipharm®; Albright & Wilson Ltd., Oldbury, UK). Half percent (w/w, Ph. Eur. grade) of magnesium stearate was added as a lubricating agent. The filler material and magnesium stearate were mixed for 5 min in a laboratory-scale mixer (Turbula T10B, Willy A. Bachofen AG Maschinenfabrik, Basle, Switzerland). After mixing, the masses were stored in controlled conditions for 3 days in a relative humidity of 55% and temperature of 22 °C. The particle sizes of the starting materials are given in Table 1.

Table 1

Mean particle sizes, upper and lower limits for powder weights and compression forces

Material	Mean particle size (μm)	Mass (mg)	Compression force (N)
Avicel® PH-101	50	203–344	1871–20627
Avicel® PH-200	180	219–348	2305–21619
Maize starch	17	246–334	4973–25791
Calipharm®	180	293–313	1695–14952
Lactose	75	300–319	1104–22382

2.2. Tableting

Tablets were compressed with an instrumented eccentric tablet machine (Korsch EK0, Erweka Apparatebau, Germany) using flat-faced punches with a diameter of 9 mm. The adjustments of the tablet machine were kept constant in all compressions in order to ensure the same speed of the upper punch and the same height of the tables in all cases. This was accomplished so that the upper punch was first adjusted to its lowest position. Then the position of the lower punch was adjusted by placing a calibration plate (height 3.000 mm) between the punches. After this the equipment was assembled. The compression speed was set to 34 rpm. The die was filled manually. The flywheel of the tablet machine was then twisted backward as long as possible (to the limit where the lower punch started to rise again). This was done to ensure that the tablet machine would have enough time to speed up to constant velocity after the motor was started. The upper and lower limits for powder weights and compression forces for different test materials used in this study are collected in Table 1.

3. Measurement of the punch displacement

Force measurement in eccentric tablet machines is very accurate and sensitive. Normally a change of less than 0.1% (10 N in a scale of 10 kN) is easily detected. In tablet compression studies, the problem is usually in the punch displacement determinations. Often the accuracy is over 10 μm .

When an empty eccentric tablet machine is running at a constant recycles per minute, the path of the upper punch as a function of time, near the maximum force, resembles a parabola. When mass is used the

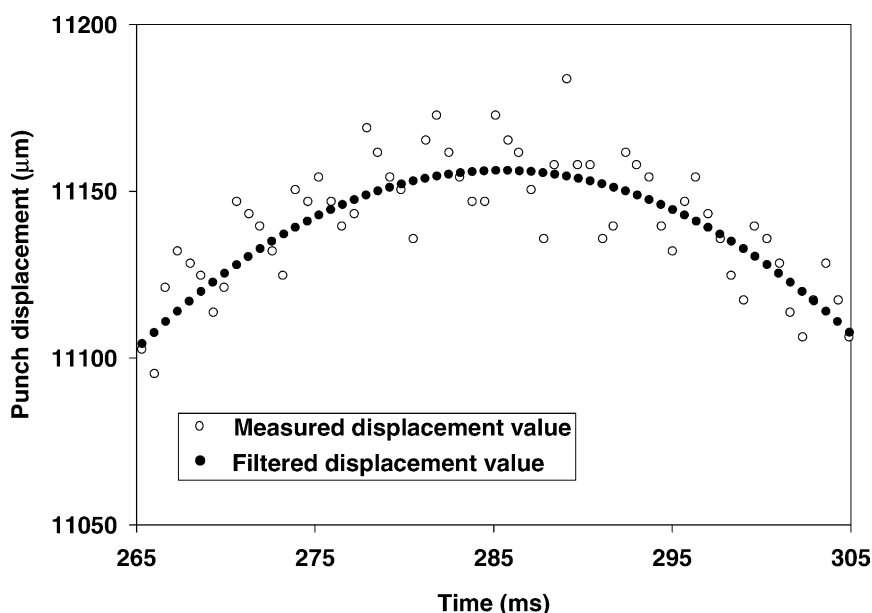


Fig. 1. Measured and filtered displacement values as a function of time.

speed of the tablet machine slows down a little at the end of the compression phase near the peak force. Therefore, in real compressions the path of the upper punch as a function of time resembles an asymmetric parabola. As a consequence of the construction of the eccentric tablet machine the real path of the upper punch as a function of time must follow the parabolic path near the peak force. Consequently, also the measured upper punch distance values as a function of time should follow this parabolic path. In this study the white noise from the displacement measurements was filtered out based on this fact. The measured distance values were used as samples to which the asymmetric parabolic curve (third-order polynomial) was fitted (Fig. 1).

4. Compression of powders

The shape of force–displacement profiles is influenced by the properties of the mass, type of tablet machine and tablet machine settings. In order to be able to compare the shape of the compression profiles of different excipients, the settings of the tablet machine must be kept constant. It is necessary to change the position of the lower punch and the path of the up-

per punch to get equal tablet weights and compression forces for different materials. If we need to adjust the upper punch to go deeper into the die, the speed of the punch changes (increases) because the punch has to move longer path in one cycle. The speed of the upper punch and the thickness of the tablet are then changed. These changes affect the shape of the compression profiles, especially the decompression phase. In this study, we filled the die manually which allowed us to keep the machine settings constant in all compressions. Then only the properties of the compressed materials caused changes in the shape of the force–distance profiles, and the changes in the machine set up did not give any extra impact. The compression force was controlled by changing the amount of powder in the die. When the amount of mass was increased, the compression forces increased. This procedure made it possible to determine deformation of the tablet machine when it was running. As the compression force increases the upper punch does not go as deep into the die as it does with lower compression forces because of the deformation in the tablet machine itself. Fig. 2 shows the path of the upper punch as a function of time with five different compression forces. The maximum displacement of the upper punch decreases as the compression force increases because of the additional deformation

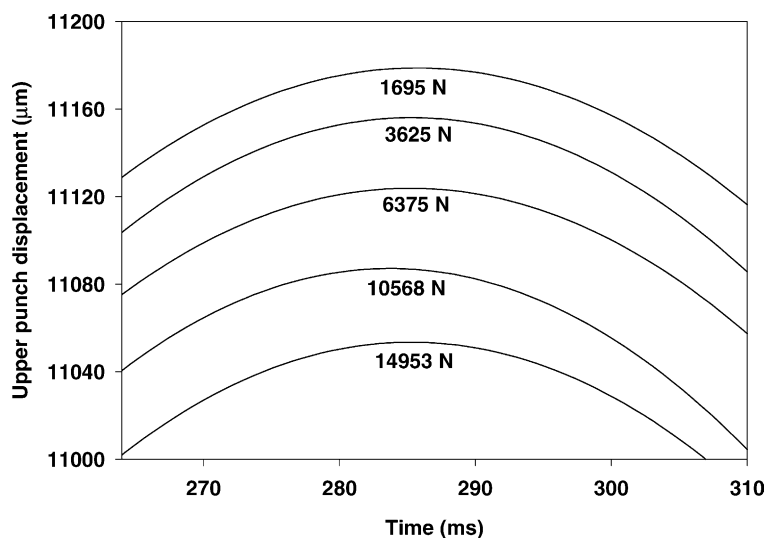


Fig. 2. Path of upper punch as a function of time with five different compression force levels.

in the machine. If there were no elastic deformation in the tablet machine at all, the upper punch would push as deep with different compression forces (different amounts of powder) because of the fixed machine set up.

Fig. 3 shows the same maximum displacement values as a function of compression force. We can see now that the maximum punch displacement decreases exponentially as the compression force is increases. A decreasing exponent curve was fitted trough these

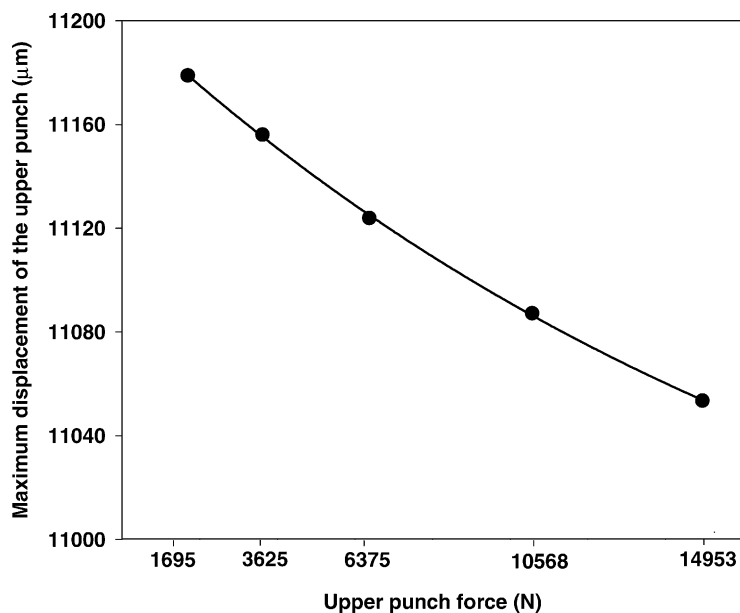


Fig. 3. Maximum displacement values as a function of compression force.

points Eq. (1).

$$s_{\max}(F) = s_{m0} + s_{df} e^{-\lambda F} \quad (1)$$

where, $s_{\max}(F)$ is the maximum displacement of the upper punch as a function of compression force; s_{m0} , minimum limit of the upper punch displacement; s_{df} , theoretical maximum limit for deformation; λ , deformation speed as the compression force increases; F is the upper punch compression force.

The values of the coefficients in Eq. (1) for $s_{df} = 281 \mu\text{m}$ and $\lambda = 5.02 \times 10^{-5} \text{ N}^{-1}$ (naturally valid for our machine only). These values will be applied in the next equation.

The deformation of the upper part of the machine (μm) as a function of upper punch compression force (N) can be calculated from the Eq. (2):

$$\text{deformation}(F) = s_{df}(1 - e^{-\lambda F}) \quad (2)$$

On the basis of Eq. (2) it was possible to determine the deformation of the upper punch and tablet machine dynamically from the running machine.

Because the lower punch is not moving during the compression phase and the machine setup was kept constant, the deformation was determined by measuring the displacement of the lower punch during maximum compression force. This displacement increased linearly as the compression force increased. The slope of the increase was $4.2 \times 10^{-3} \mu\text{m/N}$. If the compression force were for example 10 kN, the total elastic deformation of the running tablet machine in our case would be $153 \mu\text{m}$ (+111 μm for the upper punch +42 μm for the lower punch).

5. Determining the extent of plastic flow and fragmentation of powders during compression

When powder is compressed, the particles are deformed by plastic flow and brittle fracturing. Plastic flow is a time-dependent phenomenon, while fragmentation depends only on the compression pressure. The maximum compression pressure is reached before maximum punch displacement (Emschermann and Muller, 1981; Muller and Caspar, 1984; Ho and Jones, 1988). This follows from the fact that near the maximum displacement the upper punch moves very slowly and plastic materials have time to deform. If the material were totally deformed by fragmentation, this kind of phenomena would not be noticed, because

fragmentation depends on pressure, not on time. The more plastic the material is, the longer is the distance between the maximum compression pressure and the maximum displacement.

We measured material plasticity by the ratio of two areas (works) obtained from the force–distance curve near the maximum force (Eq. (5) and Fig. 4). W_1 represents an area which incontrovertibly undergoes stress relaxation in the compression phase. It is calculated using Eq. (3).

$$W_1 = \int_{s_p}^{s_{\max}} F_{\text{up}} ds - F_{s_{\max}}(s_{\max} - s_p) \quad (3)$$

W_2 describes the area that remains under W_1 in that sector of the force–distance curve.

$$W_2 = F_{s_{\max}}(s_{\max} - s_p) \quad (4)$$

where, F_{up} is the upper punch compression force; $F_{s_{\max}}$, F_{up} in maximal upper punch displacement; s_{\max} , maximal displacement of upper punch; s_p , is the displacement, when F_{up} is equal to $F_{s_{\max}}$ for the first time.

The plasticity factor PF is defined in Eq. (5). It determines the extent of plastic flow at a certain compression force level and gives a comparable numerical value.

$$\text{PF} = \left(\frac{W_1}{W_1 + W_2} \right) 100\% \quad (5)$$

6. Determining the elasticity of powders

Because of the test method described before, the thickness of the tablet and the speed of the upper punch are the same for all test materials. This makes it possible to compare reliably the elasticity of different powders. We measured the distance (s_{0d} in Fig. 5) until force due the elastic deformation of the tablet in the decompression phase was still detectable at the upper punch. It is important to know that the greatest differences in the force–displacement curves of various materials (in the decompression phase) appeared near s_{0d} . This is an area where the punch speed increases rapidly and only highly elastic materials are able to follow the punch and give a contribution to the force curve.

Thus, the elasticity factor (EF) was calculated according Eq. (6).

$$\text{EF} = \left(\frac{s_{\max} - s_{0d}}{s_{\max} - s_0} \right) 100\% \quad (6)$$

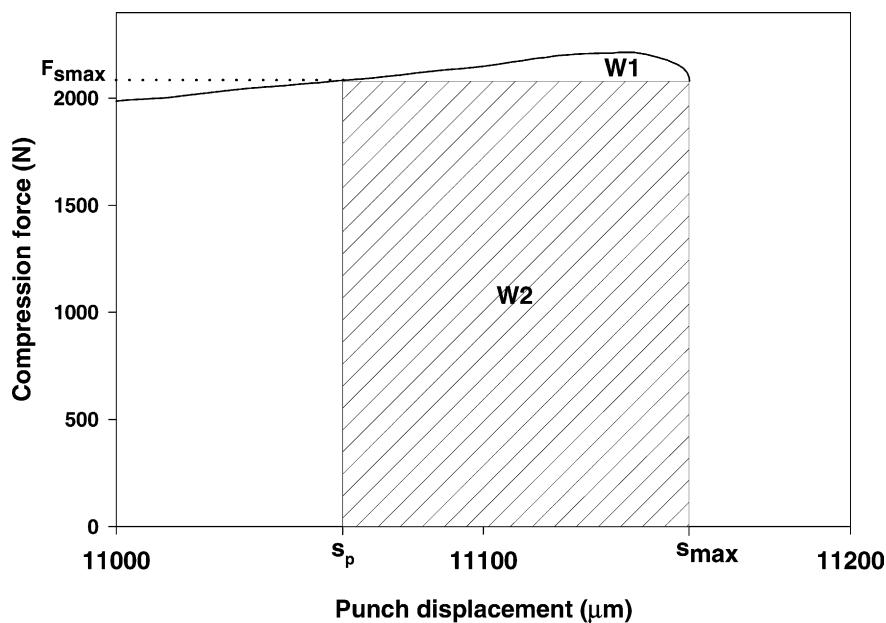


Fig. 4. Force–distance curve near maximum force.

where, s_{\max} is the maximal upper punch displacement; s_0 , displacement of upper punch when force is noticed first; s_{0d} is the displacement of the upper punch in the decompression phase when force has dropped to zero.

7. Pressure dependence of the plasticity factor PF and elasticity factor EF

The fractions of plasticity, fragmentation and elasticity are dependent of the compression pressure used.

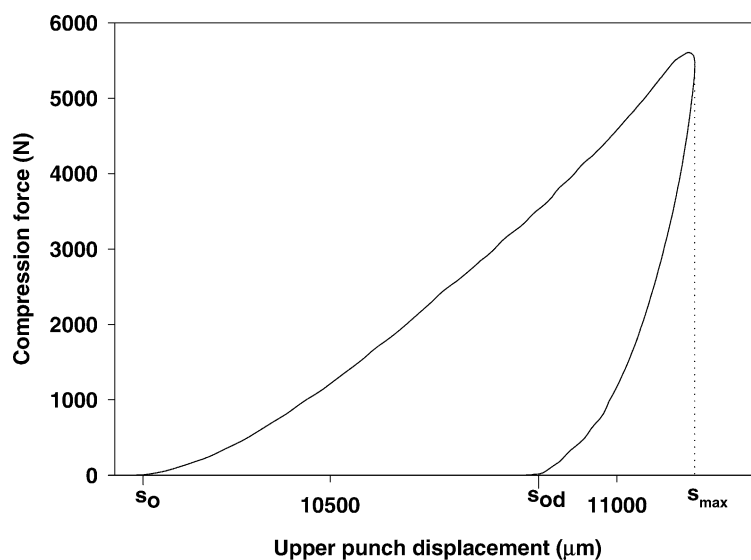


Fig. 5. Displacement values needed to calculate elasticity factor (EF).

The pressure dependence of factors PF and EF was investigated between 50 and 250 MPa (78–250 MPa for maize starch), which is a commonly used level in tablet compression.

7.1. Pressure dependence of plasticity factor PF

When we increase the compression pressure, particles that deform first by plastic flow eventually start to crack. Also when the porosity of the tablet decreases there will be less and less room for plastic flow. The PF values decreased exponentially for all materials when the compression pressure increased. Thus, the changes of PF as a function of pressure were modelled according Eq. (7).

$$PF(P) = PI e^{-v_p P} \quad (7)$$

where, PI is the theoretical maximum plasticity value at zero compression pressure; v_p is the rate at which, the plasticity decreases when the compression pressure increases.

7.2. Pressure dependence of elasticity factor EF

For microcrystalline cellulose grades and maize starch the value of EF first decreased exponentially as the pressure increased, until it reached a minimum and started to increase linearly as the pressure increased. For dicalcium phosphate dihydrate and lactose increase in only in the EF value was observed with increasing compression pressure.

The dependence of the elasticity factor EF on the compression pressure must thus be described by a combination of exponential (zero for dicalcium phosphate dihydrate and lactose) and linear function with Eq. (8).

$$EF(P) = El_1 e^{-v_{deg} P} + v_{incr} P + El_0 \quad (8)$$

where, $El_0 + El_1$ is the theoretical elasticity value at zero pressure; v_{deg} , rate at which elasticity decreases at low compression pressures; v_{incr} is the rate at which elasticity increases at high compression pressures.

8. Results and discussion

Eq. (7) presented the observed PF values satisfactorily and logically. When the pressure decreased to-

wards zero, the PF approached the maximum plasticity value PI. On the other hand, with increasing pressure the PF values decreased asymptotically towards zero. The values of PI and v_p for the tested powders are shown in Table 2.

We can see from Fig. 6 and Table 2 that dicalcium phosphate dihydrate is the least plastic material at low compression pressures (coefficient PI is the smallest) and consequently deforms mainly by fragmentation. With small pressures the rest of the test materials exhibit high PF values, but lactose turns rapidly into a brittle fracturing material as the pressure increases (coefficient v_p is clearly highest). Avicel® PH-101 maintains best its plastic feature also with high pressures (v_p is small).

The results for elasticity measurements are given in Table 3 and Fig. 7. The reason for the elasticity value of microcrystalline cellulose and maize starch first to decrease and thereafter to increase (at a certain compression level) is probably air trapped inside the tablet. For this kind of materials the risk of capping is significant in high-speed rotary tablet machines. At low compression levels (low densities) the amount of trapped air is still high. It creates a kind of “air springs” inside the tablets, which increases the elasticity values. At higher compression pressures and higher tablet densities the influence of trapped air becomes less significant, because it has already been removed from the tablets. The minimum elasticity value for Avicel® PH-101 was reached at 89.3 MPa and for Avicel® PH-200 at 90.8 MPa upper punch compression pressure. The porosity of the Avicel® tablets was then 0.17. For maize starch the same values were 167.6 MPa and 0.12. We can see from Fig. 7 that maize starch is clearly more elastic than the rest of the test materials ($El_0 + El_1$ value is highest). The elasticity value EF was especially high with

Table 2
Coefficients and degree of explanation R^2 for plasticity factor $PF(P)$ Eq. (7) (pressure in MPa)

Material	PI	$v_p \times 10^{-3} \text{ (MPa}^{-1}\text{)}$	R^2
Avicel® PH-101	5.8	9.3	0.96
Avicel® PH-200	5.7	9.5	0.97
Maize starch	6.3	10	0.95
Caliphar®	1.4	7.5	0.97
Lactose	6.2	16	0.95

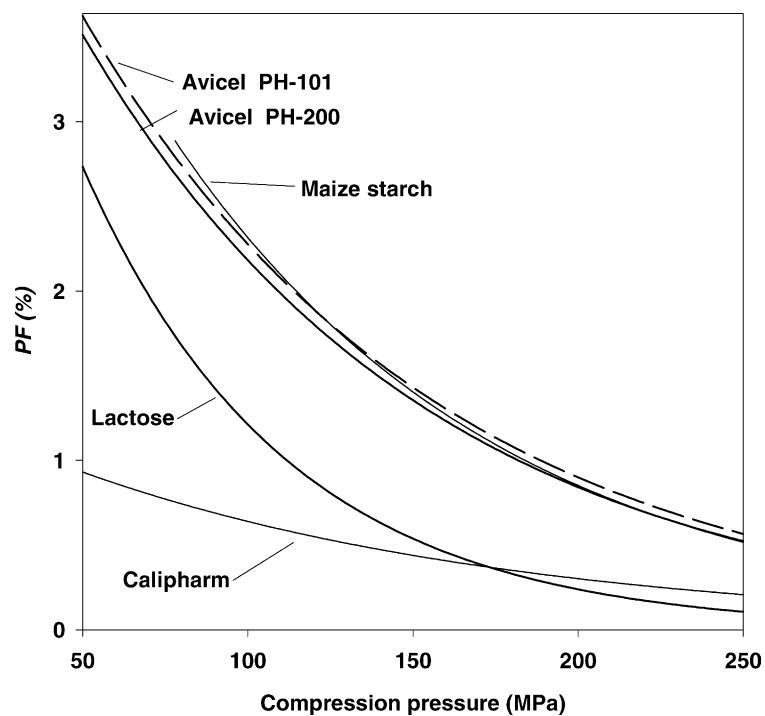


Fig. 6. Plasticity factor (PF) as a function of compression pressure for different materials.

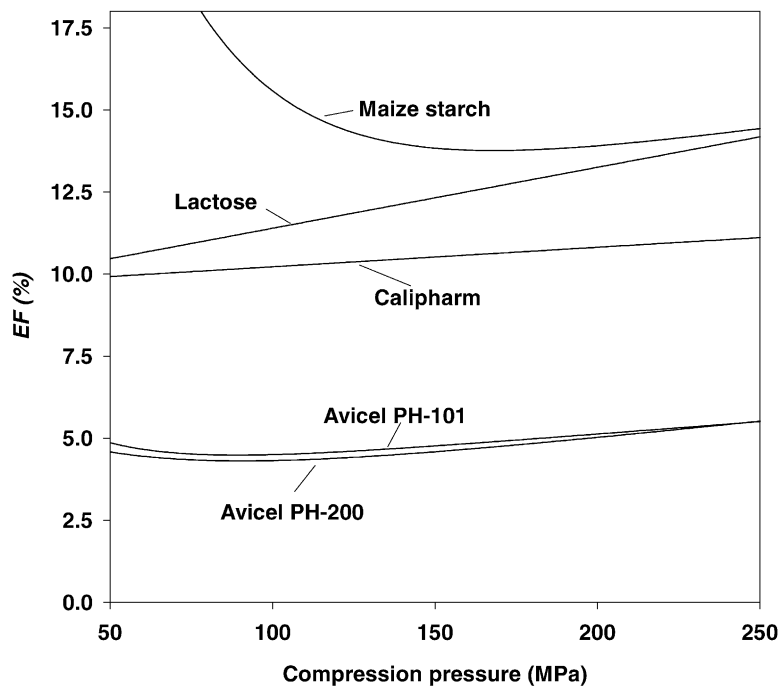


Fig. 7. Elasticity factor (EF) as a function of compression pressure for different materials.

Table 3

Coefficients and degree of explanation R^2 for elasticity factor $EF(P)$ Eq. (7) (pressure in MPa)

Material	$El_0 + El_1$	$v_{deg} \times 10^{-2} \text{ (MPa}^{-1}\text{)}$	$v_{incr} \times 10^{-3} \text{ (MPa}^{-1}\text{)}$	El_1	El_0	R^2
Avicel® PH-101	9.3	3.8	7.6	5.73	3.60	0.85
Avicel® PH-200	6.5	2.3	10	3.58	2.90	0.97
Maize starch	63	2.8	14	51.9	11.0	0.63
Caliphar®	9.6	0	6.0	0	9.62	0.95
Lactose	9.5	0	19	0	9.53	0.97

low compression pressure levels and maize starch did not form coherent tablets below 78 MPa compression pressure. EF values were lowest for microcrystalline cellulose tablets and they required the lowest compression pressure levels to form coherent tablets. The elasticity of lactose increased most rapidly as the compression pressure increased (coefficient ve_2 is highest).

9. Conclusions

By filtering the measured displacement data with the method described, its possible to remove white noise and essentially improve the accuracy of the displacement measurement.

Because the settings of the tablet machine are kept constant in all compressions, only the properties of the mass influence the shape of the force–distance curves. Above principles also make it possible to determine the deformation of an eccentric tablet machine dynamically.

The extent of plastic flow, fragmentation and elastic recovery of different powders can be determined by our method. Results are obtained as numerical values which are comparable material parameters. In addition, the pressure dependence of plastic flow, fragmentation and elastic recovery can be quantified.

References

- Armstrong, N.A., Haines-Nutt, R.F., 1970. The compaction of magnesium carbonate. *J. Pharm. Pharmacol.* 22 (Suppl.), 8S–10S.
- Cooper, A.R., Eaton, L.E.J., 1962. Compaction behavior of several ceramic powders. *Am. Ceramic Soc.* 45, 97–101.
- David, S.T., Augsburger, L.L., 1977. Plastic flow during compression of directly compressible fillers and its effect on tablet strength. *J. Pharm. Sci.* 66, 155–159.
- Dietrich, R., Mielck, J., 1983. Parametrisierung des zeitlichen Verlaufs der Verdichtung bei der Tablettierung mit Hilfe der modifizierten Weibull-Funktion. *Pharm. Ind.* 46, 863–869.
- Duberg, M., Nyström, C., 1982. Studies on direct compression of tablets. VI. Evaluation of methods for the estimation of particle fragmentation during compaction. *Acta Pharm. Suec.* 19, 421–436.
- Duberg, M., Nyström, C., 1986. Studies on direct compression of tablets. XVII. Porosity–pressure curves for the characterization of volume reduction mechanisms in powder compression. *Powder Technol.* 46, 67–75.
- Emschermann, B., Muller, F., 1981. Auswertung der kraftmessung beim tablettieren. *Pharm. Ind.* 43, 191–194.
- Hardman, J.S., Lilley, B.A., 1970. Deformation of particles during briquetting. *Nature* 228, 353–355.
- Heckel, R.W., 1961a. Density–pressure relationship in powder compaction. *Trans. Met. Soc. AIME* 221, 671–675.
- Heckel, R.W., 1961b. An analysis of powder compaction phenomena. *Trans. Met. Soc. AIME* 221, 1001–1008.
- Ho, A.Y.K., Jones, T.M., 1988. Punch travel beyond peak force during tablet compression. *J. Pharm. Pharmacol. Suppl.* 40, 75P.
- Kawakita, K., Tsutsumi, Y., 1966. A comparison of equations for powder compression. *Bull. Chem. Soc. Japan* 39, 1364–1368.
- McKenna, A., McCafferty, D.F., 1982. Effect on particle size on the compaction mechanism and tensile strength of tablets. *J. Pharm. Pharmacol.* 34, 347–351.
- Muller, F., Caspar, U., 1984. Viskoelastische phänomene während der tablettierung. *Pharm. Ind.* 46, 1049–1056.
- Pedersen, S., Kristensen, H.G., 1994. Change in crystal density of acetylsalicylic acid during compaction. *S.T.P. Pharm. Sci.* 4, 201–206.
- Roberts, R.J., Rowe, R.C., 1985. The effect of punch velocity on the compaction of a variety of materials. *J. Pharm. Pharmacol.* 37, 377–384.
- Roberts, R.J., Rowe, R.C., 1986. The effect of the relationship between punch velocity and particle size on the compaction behavior of materials with varying deformation mechanisms. *J. Pharm. Pharmacol.* 38, 567–571.
- Roberts, R.J., Rowe, R.C., 1987. The Young's modulus of pharmaceutical materials. *Int. J. Pharm.* 37, 15–18.
- Sonnergaard, J.M., 1999. A critical evaluation of the Heckel equation. *Int. J. Pharm.* 193, 63–71.
- Watt, P., 1988. *Tablet Machine Instrumentation in Pharmaceutics: Principles and Practice*. Ellis Horwood Limited, Chichester.